

***Cell*, Volume 133**

Supplemental Data

The 3D Structure of the Immunoglobulin

Heavy-Chain Locus: Implications

for Long-Range Genomic Interactions

Suchit Jhunjhunwala, Menno C. van Zelm, Mandy M. Peak, Steve Cutchin, Roy Riblet, Jacques J. M. van Dongen, Frank G. Grosveld, Tobias A. Knoch, and Cornelis Murre

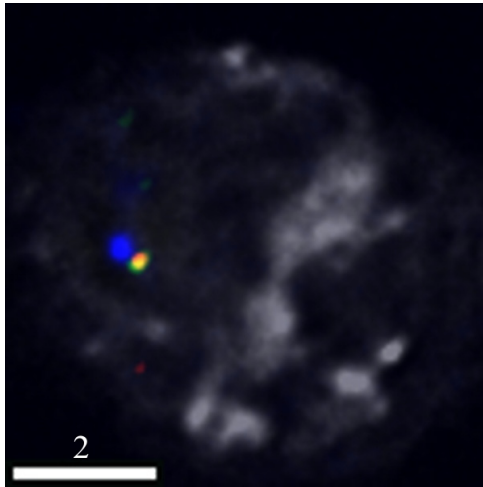
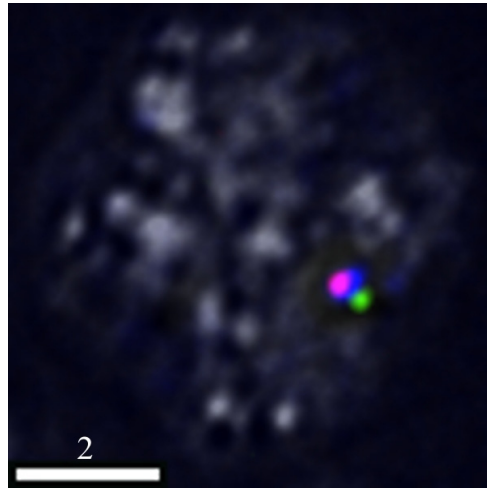
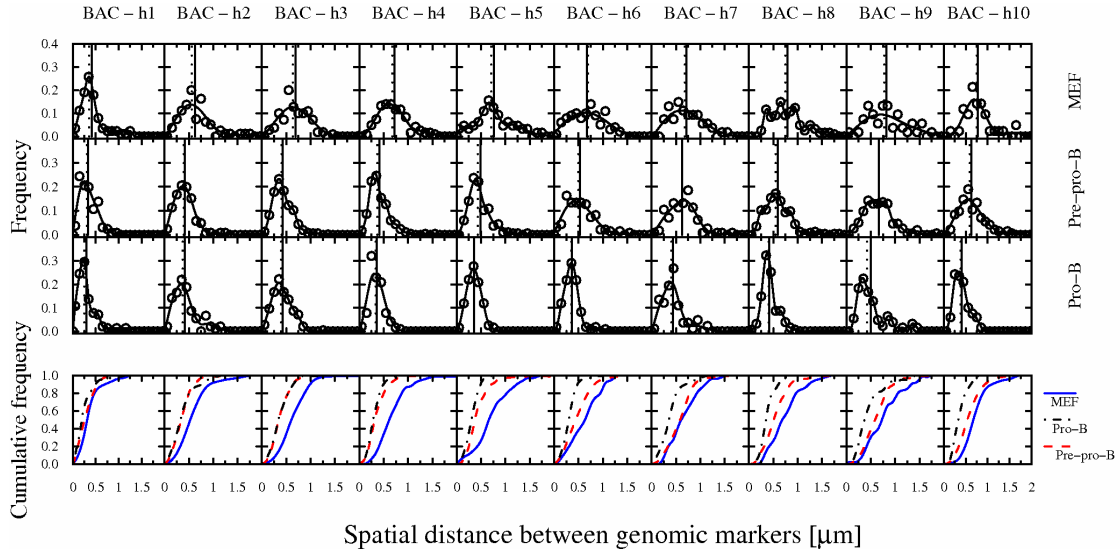


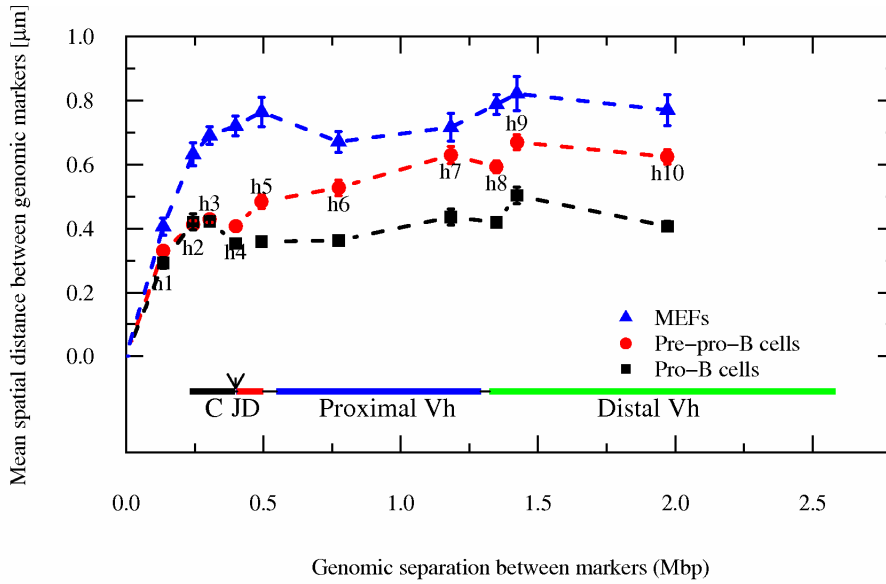
Figure S1. 3D-Structure Preserving-Fluorescence *in situ* Hybridization and Spectral Precision Distance Epifluorescence Microscopy

Three-dimensional fluorescence *in situ* hybridization in nuclei derived from RAG2-deficient pro-B cells using 10 kbp probes. Digitally magnified pictures of the Igh locus are shown. Two 10 kbp-probes (shown in red and green) were labelled with aminoallyl-dUTP using nick-translation followed by incubation with succinimidyl-ester conjugates of Alexa fluorochromes. Nuclei are visualized by DAPI staining.

A



B



C

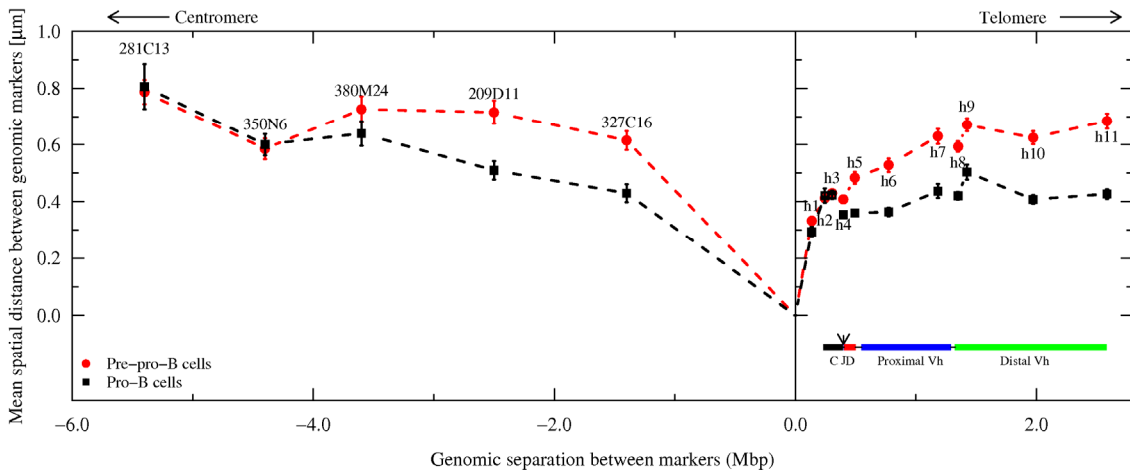


Figure S2. Immunoglobulin Heavy Chain Locus Spatial Distances and Spatial Distributions as a Function of Genomic Separation in Murine Embryonic Fibroblasts cells, Pre-Pro-B and Pro-B Cells

(A) Frequency plots showing the distribution of spatial distances between probes and the anchor (RP23-201H14). Cumulative frequency distributions are indicated for murine embryonic fibroblasts, pre-pro-B and pro-B cells.

(B) Average spatial distances were plotted as a function of genomic separation for murine embryonic fibroblasts (MEFs), pre-pro-B and pro-B cells. Spatial distances were measured using RP23-201H14 as an anchor as a function of genomic separation towards the telomere. Distal and proximal variable regions as well as diversity, joining and constant region segments are shown. Bars indicate standard error of the mean. The arrow indicates the position of the intronic enhancer.

(C) Average spatial distances were plotted as a function of genomic separation for pre-pro-B and pro-B cells. Spatial distances were measured using RP23-201H14 as an anchor as a function of genomic separation towards both the telomere and centromere. Distal and proximal variable regions as well as diversity, joining and constant region segments are shown. Bars indicate standard error of the mean. The arrow indicates the position of the intronic enhancer.

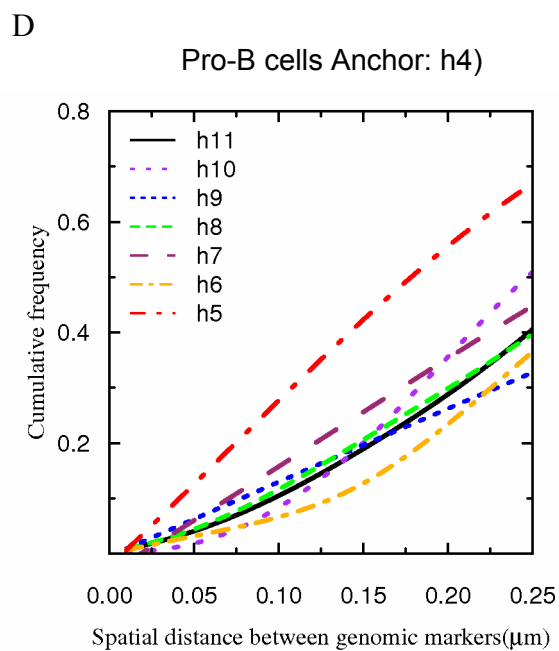
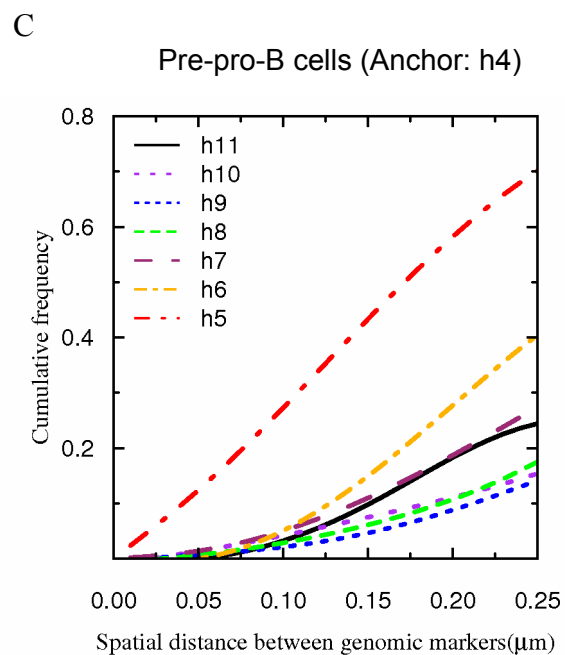
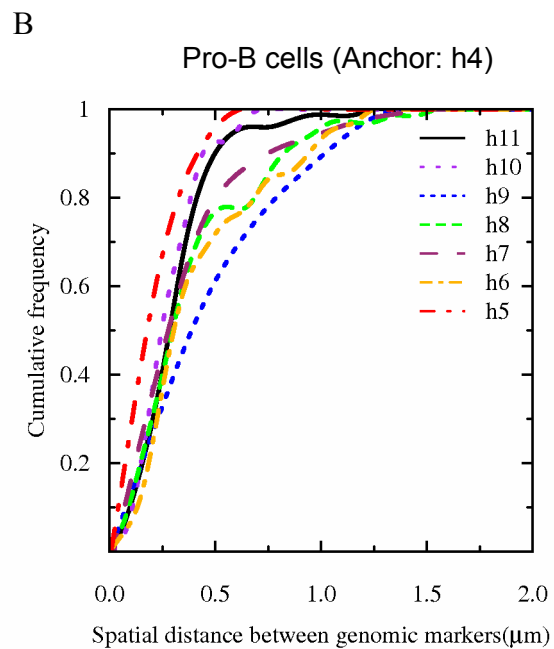
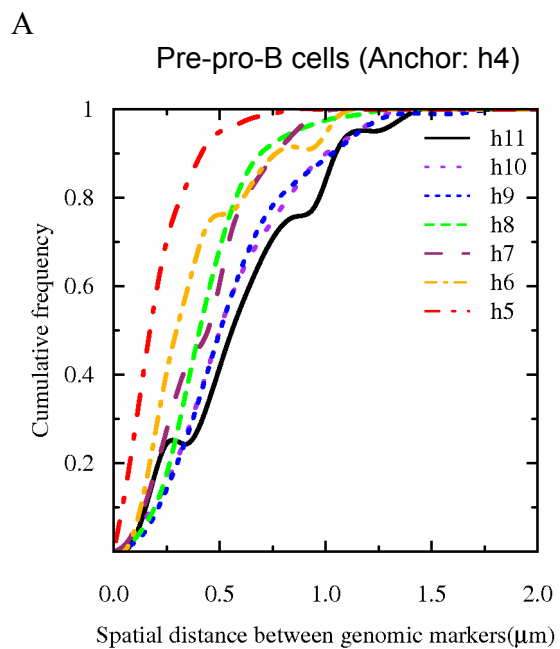


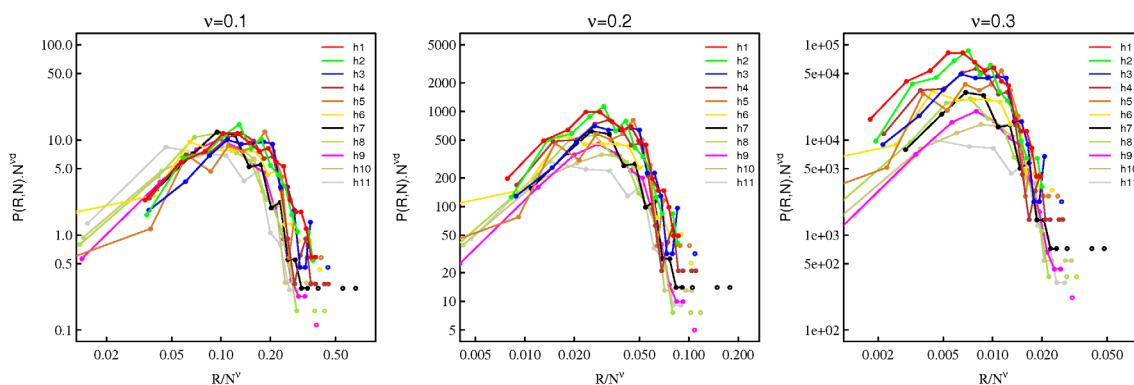
Figure S3. Cumulative Frequency Distributions as a Function of Genomic Separation

(A) Probabilities for proximal and distal V_H regions to be in spatial proximity to the D_HJ_H elements in pre-pro-B cells. Cumulative frequencies were obtained by accumulating the frequency values corresponding to the spatial distances in intervals of 100 nm using the D_HJ_H elements (probe h4) as an anchor.

(B) Probabilities for V_H regions to be in spatial proximity to the D_HJ_H elements in pro-B cells. Cumulative frequencies were obtained by accumulating the frequency values corresponding to the spatial distances in intervals of 100 nm using the D_HJ_H elements (probe h4) as an anchor.

(C and D) Cumulative frequency distributions separating V_H from D_HJ_H elements in pre-pro-B (C) and pro-B cells (D) were plotted for spatial distances separated by less than 250 nm.

Pre-pro-B cells



Pro-B cells, distances from BAC

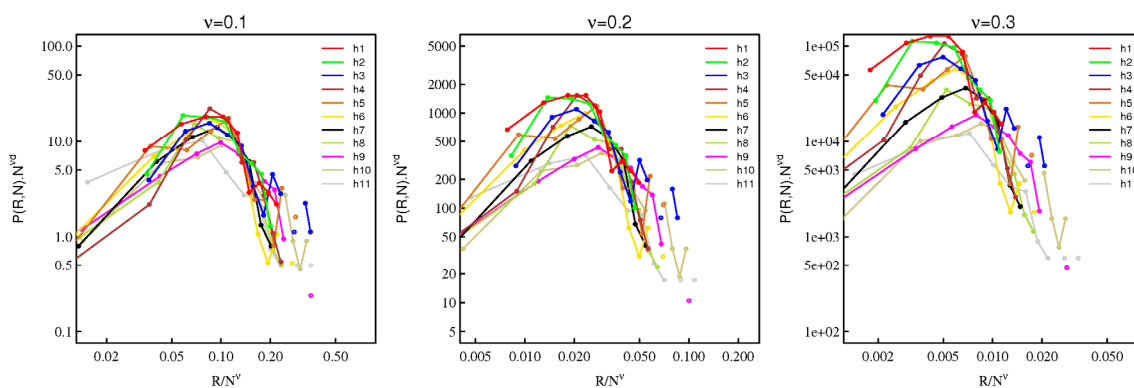
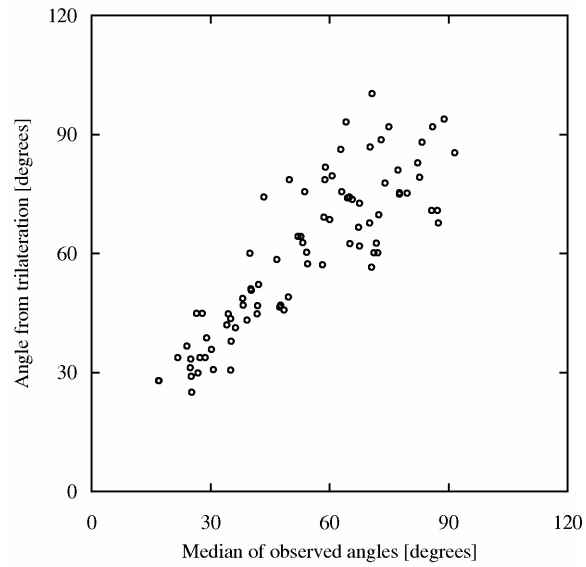


Figure S4. Scaled Distribution of Spatial Distances Plotted for Comparison with a Self-Avoiding Random Walk

Probability (P) that two genomic markers separated by ' N ' basepairs are at a spatial distance ' R ' is indicated. ' d ' refers to the number of dimensions ($d=3$). Different values for the exponent v (which has the value ~ 0.6 for a self avoiding random walk) were tested. At lower values of v (below 0.3), the curves are closer to each other than they are at $n = 0.6$. Graphs are shown for both cell types, and with the BAC probe as the anchor.

A



B

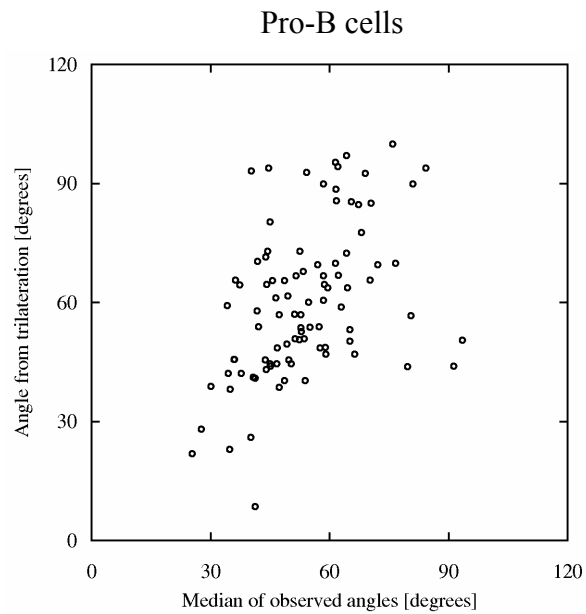
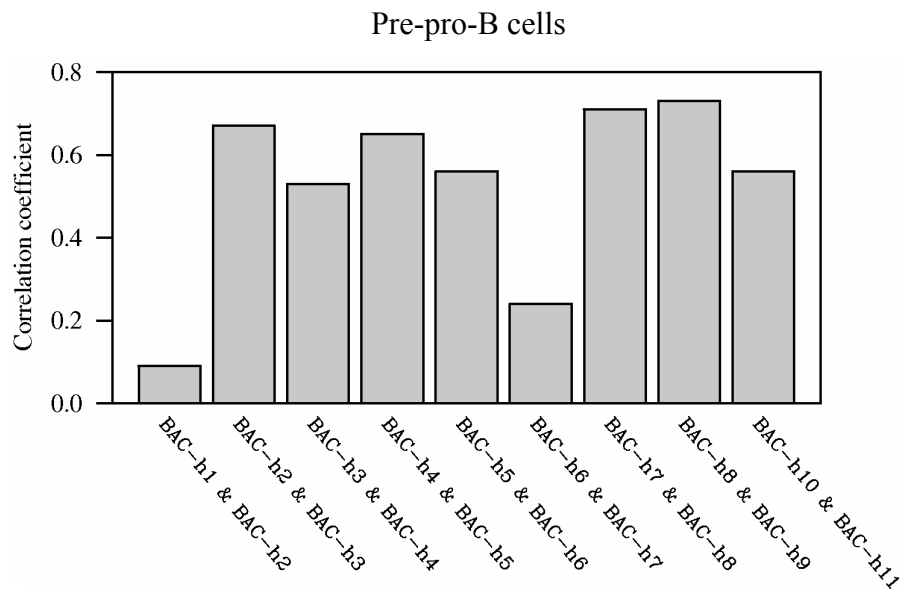


Figure S5. Comparison of Angles Derived From Three Point Measurements and Trilateration

(A-B) The distribution of angles for different combinations for three probes was determined and the median angles that were observed were compared to those obtained using trilateration.

A



B

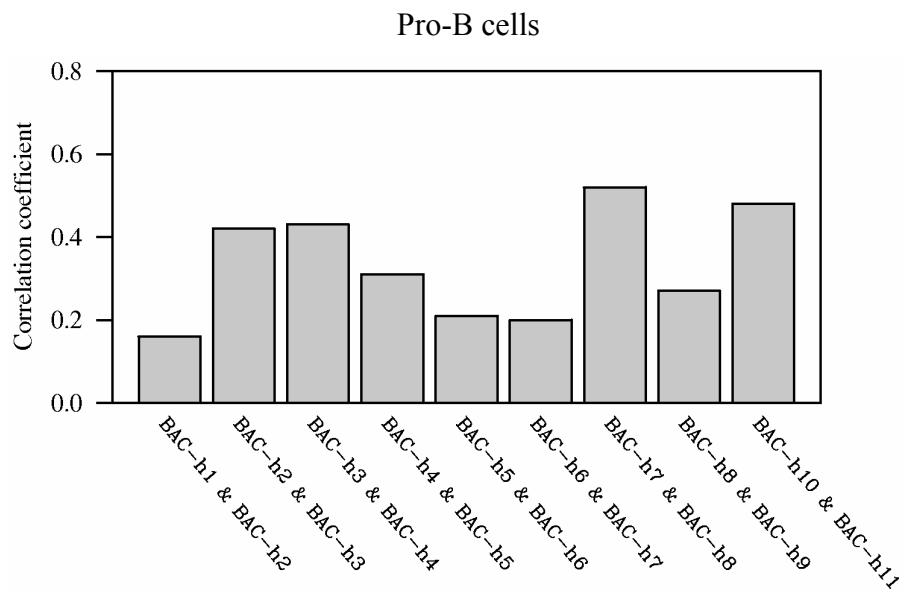


Figure S6. DNA Elements within a Chromatin Compartment are Relatively Fixed

Correlation Coefficients were computed for spatial distances separating two consecutive genomic markers from an anchor located in a distinct chromatin territory. Correlation coefficients for both pre-pro-B (A) and pro-B (B) cells are shown.

Table S1. Average spatial distances and chromatin compaction as a function of genomic separation in the immunoglobulin heavy chain locus

Marker Pair	Genomic Separation [Mbp]	Pre-pro-B cells				Pro-B cells			
		Detection	Nuclei [N]	Spatial Distance <d> ± SD ± SE [nm]	Com- paction	Detection	Nuclei [N]	Spatial Distance <d> ± SD ± SE [nm]	Com- paction
BAC - h1	0.14	A647 / A488	131	331.6 ± 181.4 ± 15.8	138	A647/ A488	139	293.2 ± 199.2 ± 16.9	156
BAC - h2	0.24	A647 / A594	262	412.4 ± 203.6 ± 12.6	201	A647 / A594	91	421.1 ± 236.5 ± 24.8	197
BAC - h3	0.30	A647 / A488	391	429.4 ± 196.9 ± 10.0	241	A647 / A488	185	423.4 ± 194.0 ± 14.3	244
BAC - h4	0.40	A647 / A594	300	408.1 ± 206.5 ± 11.9	332	A647 / A594	193	354.1 ± 147.1 ± 10.6	382
BAC - h5	0.49	A647 / A488	185	483.9 ± 286.1 ± 21.0	346	A647 / A488	192	360.2 ± 139.3 ± 10.1	465
BAC - h6	0.77	A647 / A594	135	528.1 ± 278.8 ± 24.0	498	A647 / A594	110	363.4 ± 158.9 ± 15.1	724
BAC - h7	1.18	A647 / A594	114	630.0 ± 278.2 ± 26.1	638	A647 / A594	82	436.8 ± 227.1 ± 25.1	920
BAC - h8	1.35	A647 / A488	227	593.8 ± 278.6 ± 18.5	772	A647 / A488	127	420.3 ± 154.8 ± 13.7	1091
BAC - h9	1.42	A647 / A594	154	670.4 ± 284.9 ± 23.0	722	A647 / A594	125	504.0 ± 293.5 ± 26.2	960
BAC - h10	1.97	A647 / A488	143	624.5 ± 275.0 ± 23.0	1073	A647 / A488	119	407.7 ± 164.9 ± 15.1	1644
BAC - h11	2.59	A647 / A594	143	684.4 ± 317.4 ± 26.5	1284	A647 / A594	115	426.8 ± 185.5 ± 17.3	2059
h4 - h1	0.26	A594 / A488	94	350.1 ± 155.4 ± 16.0	256	A488 / A594	58	440.0 ± 251.4 ± 33.0	204
h4 - h2	0.16	A488 / A594	100	246.0 ± 150.8 ± 15.1	214	A488 / A594	59	357.8 ± 256.6 ± 33.4	147
h4 - h3	0.09	A594 / A488	188	258.8 ± 161.9 ± 11.8	124	A488 / A594	67	337.4 ± 241.5 ± 29.5	95
h4 - h5	0.10	A594 / A488	97	252.3 ± 155.9 ± 15.8	128	A594 / A488	38	255.5 ± 140.7 ± 22.8	126
h4 - h6	0.38	A488 / A594	47	436.0 ± 260.3 ± 38.0	293	A488 / A594	63	465.6 ± 310.7 ± 39.1	274
h4 - h7	0.78	A488 / A594	73	479.4 ± 233.0 ± 27.3	556	A488 / A594	55	407.5 ± 287.5 ± 38.8	654
h4 - h8	0.95	A594 / A488	59	483.5 ± 227.5 ± 29.6	668	A594 / A488	68	440.0 ± 309.6 ± 37.5	734
h4 - h9	1.03	A488 / A594	93	609.8 ± 307.0 ± 31.8	450	A488 / A594	42	524.3 ± 336.8 ± 52.0	665
h4 - h10	1.57	A488 / A594	70	607.2 ± 301.6 ± 36.1	881	A488 / A594	55	325.7 ± 145.7 ± 19.6	1642
h4 - h11	2.19	A488 / A594	41	641.9 ± 346.7 ± 54.1	1158	A488 / A594	74	353.5 ± 194.1 ± 22.6	2103

n refers to number of alleles analyzed. SD indicates standard deviation. SE refers to standard error. <x> indicates average spatial distance. The average DNA compaction based on the linear contour length of 340 nm for 1.0 kbp was calculated as follows:

$$\text{Compaction value} = \frac{340 \text{ [nm]} \cdot (\text{genomic length [kb]})}{(\text{spatial distance [nm]}) \cdot [\text{kb}]}$$

Table S2. Full width at half the maximum (FWHM) values for the Point Spread Function (PSF) for each color. All values are in nanometers.

<i>Color</i>	FWHM _x [nm]	FWHM _y [nm]	FWHM _z [nm]
<i>A 488</i>	543	489	1800
<i>A 594</i>	380	380	1400
<i>A 647</i>	434	434	1700

Table S3. Chromatic shift c between different fluorophores and resolution equivalents RE before (RE_b) and after (RE_a) applying chromatic corrections. ‘A’ indicates Alexa fluorochromes.

Colors	A 488 / A 594	A 488 / A 647	A 594 / A 647
Number of Distances [N]	226	226	226
$\langle c_x \rangle \pm \sigma \pm \Delta$ [nm]	$+31.7 \pm 16.5 \pm 1.1$	$+53.5 \pm 30.2 \pm 2.0$	$-21.8 \pm 22.9 \pm 1.5$
$\langle c_y \rangle \pm \sigma \pm \Delta$ [nm]	$-14.4 \pm 17.2 \pm 1.1$	$-2.8 \pm 31.5 \pm 2.1$	$-11.6 \pm 25.0 \pm 1.7$
$\langle c_z \rangle \pm \sigma \pm \Delta$ [nm]	$-133.0 \pm 35.3 \pm 2.3$	$-159.1 \pm 24.9 \pm 1.7$	$+26.1 \pm 36.6 \pm 2.4$
$\langle RE_b \rangle \pm \sigma \pm \Delta$ [nm]	$139.7 \pm 34.6 \pm 2.3$	$173.2 \pm 26.2 \pm 1.7$	$56.3 \pm 24.6 \pm 1.6$
$\langle RE_a \rangle \pm \sigma \pm \Delta$ [nm]	$34.9 \pm 24.3 \pm 1.6$	$46.8 \pm 17.8 \pm 1.2$	$44.6 \pm 22.1 \pm 1.5$

Table S4. Average spatial distances [μm] separating genomic markers spanning the entire immunoglobulin heavy chain locus in pre-pro-B and pro-B cells

		— Pre-pro B cells →												
← Pro-B cells —		BAC	h1	h2	h3	h4	h5	h6	H7	h8	h9	h10	h11	
		BAC		0.3117	0.4128	0.4401	0.4027	0.4350	0.5040	0.5958	0.5351	0.6568	0.5900	0.6059
		h1	0.2788		0.3793	0.3903	0.3348							
		h2	0.3936	0.4182		0.2401	0.2471	0.2799						
		h3	0.4578	0.4757	0.3229		0.2471	0.2687	0.3643	0.5847	0.4141	0.5287	0.5769	0.6433
		h4	0.3378	0.4013	0.3453	0.3353		0.2638	0.4082	0.4631	0.4504	0.7461	0.5726	0.6364
		h5	0.3882			0.3580	0.2589		0.3407					
		h6	0.3512			0.3698	0.4189	0.2876		0.4697				
		h7	0.4009			0.4192	0.3479		0.3722		0.3243			
		h8	0.4208			0.4407	0.4165			0.2944		0.2535	0.3582	0.4093
		h9	0.4519			0.3884	0.5249				0.3239			
		h10	0.4167			0.4107	0.3226					0.4223		0.3435
		h11	0.4086			0.4184	0.3275						0.2540	

Spatial distances were determined between genomic markers using 3D-FISH and epifluorescence microscopy. Both pre-pro-B and pro-B cells were analyzed. Distances separating the various probes are indicated in the matrix and analyzed using trilateration.

Table S5: 3D-coordinates of the hybridization probes obtained by trilateration before and after error reduction.

Pre-pro-B cells:

Probe	x	Y	z	Error
BAC	0.0000	0.0000	0.0000	0.0000
H01	0.1573	0.1148	-0.2434	0.0539
H02	0.3481	0.1729	0.1389	0.1164
H03	0.4401	0.0000	0.0000	0.0267
H04	0.3349	0.2236	0.0000	0.1910
H05	0.3530	0.1851	-0.1743	0.1883
H06	0.3579	0.1337	0.3287	0.2888
H07	0.2350	0.2951	0.4612	0.2407
H08	0.3749	0.1164	0.3636	0.2260
H09	0.3926	-0.2070	0.4842	0.3829
H10	0.2374	0.1139	0.5280	0.4605
H11	0.1670	0.0740	0.5777	0.2691

After error reduction:

Probe	x	Y	z	Error
BAC	0.0103	-0.0084	-0.0005	0.0679
H01	0.1374	0.1242	-0.2349	0.0524
H02	0.3553	0.1155	0.1226	0.0699
H03	0.4176	-0.0027	-0.0338	0.1521
H04	0.2834	0.2694	0.0008	0.1357
H05	0.4170	0.1599	-0.1436	0.1061
H06	0.4883	0.0314	0.2303	0.1169
H07	0.2243	0.3031	0.4538	0.0398
H08	0.4394	0.0643	0.3564	0.0848
H09	0.3926	-0.2070	0.4842	0.1109
H10	0.3226	-0.1990	0.4624	0.1294
H11	0.1341	0.0599	0.5767	0.0444

Pro-B cells:

Probe	x	Y	z	Error
BAC	0.0000	0.0000	0.0000	0.0000
H01	0.0666	-0.0045	-0.2707	0.1619
H02	0.2793	0.0161	0.2686	0.2110
H03	0.4578	0.0000	0.0000	0.0205
H04	0.2307	0.2467	0.0000	0.0252
H05	0.2535	0.1574	0.2482	0.1378
H06	0.2143	-0.0949	0.2616	0.1705
H07	0.2068	0.1008	0.3203	0.2777
H08	0.1900	0.0517	0.3718	0.4393
H09	0.2872	-0.2143	0.2754	0.0620
H10	0.2344	0.1474	0.3114	0.3375
H11	0.2169	0.1385	0.3128	0.3767

After error reduction:

Probe	x	Y	z	Error
BAC	-0.0193	0.0788	-0.0168	0.0777
H01	0.0687	-0.0422	-0.2492	0.0048
H02	0.2427	-0.1460	0.1181	0.0381
H03	0.4659	0.0231	-0.0010	0.0887
H04	0.2440	0.2106	0.0125	0.0937
H05	0.2391	0.0853	0.2569	0.0309
H06	0.1811	-0.1808	0.1232	0.0269
H07	0.1980	0.1121	0.3254	0.0293
H08	0.1170	-0.1642	0.2426	0.1002
H09	0.2608	-0.2941	0.0341	0.0589
H10	0.2808	0.0686	0.3107	0.1072
H11	0.1936	0.2458	0.2936	0.0816

Supplemental Experimental Procedures

High-Resolution 3D-Structure Preserving Fluorescence in situ Hybridization

40 μ l of a 1×10^6 cells/ml suspension of cells was directly attached to coverslips. Cells were fixed in 4% paraformaldehyde for 10 min. at room temperature and carefully placed on a coverslip. Next, cells were incubated with 0.1M Tris-Cl pH7.2 for 10 min. at room temperature and the coverslips were washed with 1X Phosphate buffer saline (PBS). Cells were permeabilized for 10 min. at room temperature with PBS plus 0.1% triton x-100 and 0.1% saponin and then incubated for 20 minutes with 20% glycerol/1X PBS. Subsequently, coverslips were immersed in liquid nitrogen and thawed for three consecutive times. Cells were washed once in PBS, then treated for 30 minutes with a 0.1 N HCl solution at room temperature, washed once in PBS, and incubated with 100 μ g/ml DNase-free RNase in 3% bovine serum albumin (BSA) / 0.1% triton X-100 for 1 hour at 37 °C. Cells were again permeabilized in PBS, 0.5% triton X-100, 0.5% saponin solution for 30 minutes at room temperature. Cells were then washed once in PBS. Nuclear DNA was denatured by incubating coverslips for 2 minutes and 30 seconds at 73 °C in 2X SSC, 70% formamide solution followed by an incubation of 1 minute in 2X SSC plus 50% formamide. Excess liquid was removed and 10 μ l of hybridization cocktail was added to each of the coverslips. Coverslips were mounted, sealed with rubber-cement, and incubated overnight at 37 °C. The hybridization solution contained 400 ng of labeled BAC probe, 40 ng each of labeled 10kbp probes, 4 μ g of mouse Cot -1 DNA, 1 μ g of sheared salmon-sperm DNA dissolved in 50% formamide, 4XSSC and 20% dextran sulfate. The probes were denatured at 75°C for 5 minutes and chilled on ice

prior to incubation with coverslips. On the following day, coverslips were removed and washed once in 2X SSC and 50% formamide for 15 minutes and 3 times in 2X SSC for a 5 minute period at 37 °C with low agitation (100 rpm). Cells were washed once with PBS, excess PBS was removed and coverslips were mounted on slides with 12 μ l of Prolong gold anti-fade reagent (Invitrogen) and 400 ng/ml DAPI.

Image Acquisitions, Distance Calculations, Calibration and Statistics

Images were captured with a DeltaVision epifluorescent deconvolution microscope system (Applied Precision, Inc.) located at the UCSD cancer centre microscope facility. Using a 100x (NA 1.4) lens, images of approximately 40 serial optical sections spaced by 0.2 μ m were acquired from experiments involving BAC DNA probes only, and 80 serial optical sections spaced by 0.1 μ m were acquired from experiments involving 10kb DNA probes. To achieve high precision and analytical correction of the optics the point spread function (PSF) with its full width at half the maximum (FWHM) and the chromatic shift between the fluorophores was measured with fluorescently labeled tetraspeck beads (Invitrogen, 0.2 μ m) at 0.1 μ m z-intervals. Each bead was uniformly stained with a mixture of fluorescent dyes that emit in the blue, green, orange and dark red wavelengths.

For chromatic shift correction, determination of the resolution equivalent and the experimental measurements, the image stacks were deconvolved and optical sections were merged to produce 3D-pictures using SoftWorx software (Applied Precision, Inc) on a Silicon Graphics Octane workstation. The 3D-

coordinates of the center of mass of each probe were obtained. The chromatic shift was determined by subtraction of the individual center of mass coordinates of the same bead observed under different colors.

To determine the experimental spatial distances, the initial spatial positions of signals were corrected for the chromatic shift. The average DNA compaction based on the linear contour length of 340 nm for 1.0 kbp was calculated from

$$\frac{340 \text{ [nm]} \cdot (\text{genomic length [kb]})}{(\langle \text{spatial distance} \rangle \text{ [nm]}) \cdot 1 \text{ [kb]}}$$

To determine the smallest measurable distance that we could observe using spectral precision epifluorescence microscopy, we measured the point spread function (PSF) and the resolution equivalent. The full width at half maximum values was determined for each fluorescent color from the PSF (lateral 380 to 542 nm, axial 1400 to 1700nm; Table S1; see Materials and Methods Section in the Supplemental Data). The approach required correction for chromatic shifts for each of the fluorophore combinations (chromatic shifts: lateral -14 to 53nm, axial -159 to 26 nm; Table S2). From this analysis the smallest measurable distances, the RE values, were determined by correcting for chromatic shifts the positions of the beads used to measure the chromatic shifts. *RE* (and also the spatial distance *d*) was then calculated according to the equation: *RE* or $d = \sqrt{(x_a - x_b)^2 + (y_a - y_b)^2 + (z_a - z_b)^2}$ with the coordinates *x*, *y*, and *z* of objects *a* and *b*. From these observations the average values were calculated (See Supplemental Table S3). The RE values ranged from 35 to 47 nm, for each of the fluorophore combinations, allowing the measurement of spatial distances with a 3D-resolution greater than 50 nm.

Computer Simulations

Using a two step combined Monte Carlo and Brownian Dynamics method, the Random-Walk/Giant-Loop (RW/GL) model (Sachs *et al.*, 1995) and the Multi Loop Subcompartment (MLS) model (Münkel & Langowski, 1998) were simulated for human interphase chromosome 15 (Knoch *et al.*, 2000; Knoch, 2002; Knoch, 2003). Assuming a flexible polymer chain, the chromatin fiber was split into ~3,300 segments of 300 nm (~31 kbp). To each segment a harmonic stretching potential and between two segments a harmonic bending potential were assigned. To avoid self-crossing of the polymer chain, a short ranged excluded volume potential was introduced, whose potential barrier could be changed to facilitate chain dis-entanglement to speed up simulations. In vivo this is mediated by Topoisomerase-II especially during chromosome de- or condensation. The simulation of single chromosomes necessitated placement into an embedding potential simulating the surrounding nuclear chromosomes. In the RW/GL model loops of 5.0, 4.0, 3.0, 2.0, 1.0, 0.504 and 0.252 Mbp were used and connected by a chromatin linker whose length was adjusted such that the global territory behavior yielded comparable results as in the MLS model. In the MLS model the loop size was 126 kbp with linker sizes of 63, 126, 189 and 252 kb. The number of loops in the rosettes varied, since the DNA content of the rosettes was assumed to be that of the metaphase ideogram banding pattern (Franke, 1994) divided by three to account for the transition into interphase ideogram bands (Yunis, 1981). The starting configuration of a chromosome had the approximate form and size of a metaphase-chromosome whose de-condensation resembles the natural process. Typically ~400,000 Monte Carlo steps were needed to

generate enough statistically independent configurations at thermodynamic equilibrium. For comparison with experimental spatial distance measurements between genetic markers as function of their genetic separation, 100 to 150 statistically independent Monte Carlo configurations were taken as starting points for relaxation at higher spatial resolution by Brownian Dynamics methods using a decreased segment length of 50 nm (~5.2 kb), corresponding to 20,000 segments for chromosome 15. 2,000 Brownian Dynamics steps were performed until equilibration was reached again. The simulated spatial distances were determined position dependently, i.e. the marker pairs were placed in respect to the topological folding of the simulated chromosome and position independently, i.e. the pairs of markers were placed randomly and therefore regardless of any folding topology on the chromosome (for the underlying assumption see results). All pairs of positions for one genomic separation were taken, the resulting spatial distance determined and averaged over 100 to 150 statistically independent chromosome configurations.

Trilateration Procedure

The BAC probe was assigned as the origin (0,0,0). Probe h3 was placed on the X-axis with the coordinates as (d_{0,3},0,0), where d_{0,3} is the spatial distance between the BAC and h3. Probe h4 was placed in the XY plane and had the coordinates as (x₄,y₄,0). The x and y coordinates of the probe h4 were calculated as follows:

$$x_4 = \frac{d_{0,3}^2 + d_{0,4}^2 - d_{3,4}^2}{2d_{0,3}}$$

$$y_4 = \sqrt{d_{0,4}^2 - x_4^2}$$

where $d_{0,4}$ is the distance of h4 from the BAC, and $d_{3,4}$ is the distance of h4 from probe h3.

The initial estimates of the x, y and z coordinates of a (non-reference) probe i were calculated as follows:

$$x_i = \frac{d_{i,0}^2 - d_{i,3}^2 + x_3^2}{2x_3}$$

$$y_i = \frac{d_{i,0}^2 - d_{i,4}^2 - 2x_i x_4 + x_4^2 + y_4^2}{2y_4}$$

$$z_i = \pm \sqrt{d_{0,i}^2 - x_i^2 - y_i^2}$$

where $d_{i,0}$, $d_{i,3}$ and $d_{i,4}$ are the 3D-distances of probe i from the reference probes BAC, h3 and h4 respectively.

The error in the estimated position of a probe i was determined as follows:

$$\sum_{\substack{j=0 \\ j \neq i}}^{11} (r_{i,j} - d_{i,j})^2$$

where $r_{i,j}$ is the distance between the probes i and j based on the 3D-coordinates of these probes, and $d_{i,j}$ is the experimental spatial distance measured for this probe pair. Only the probe-pairs for which we had an experimental spatial distance measurement were considered for error calculation. Thereafter, we used a mutiple steepest descent algorithm to iteratively change the 3D-coordinates in order to obtain the set of 3D-coordinates that substantially reduce the error associated with each probe.